World Academy of Science, Engineering and Technology
International Journal of Electronics and Communication Engineering
Vol:9, No:12, 2015

Energy Management System in Fuel Cell, Ultracapacitor, Battery Hybrid Energy Storage

Vinod Tejwani, Bhavik Suthar

Abstract**—**The paper presents and energy management strategy for a Fuel Cell, Ultracapacitor, Battery hybrid energy storage. The fuel cell hybrid power system is devised basically for emergency power requirements and transient load applications. The power density of an Ultracapacitor is extremely high and for a battery, it is subtle. For a fuel cell, the value of power density is medium. The energy density of these three stockpiling gadgets is contrarily about the power density, i.e. for the batteries it is most noteworthy and for the Ultracapacitor, it is least. Again the fuel cell has medium energy density. The proposed Energy Management System (EMS) is trying to rationalize these parameters viz. the energy density and power density. The working of the fuel cell, Ultracapacitor and batteries are controlled in a coordinated environment in a way to optimize the energy usage and at the same time to get benefits of power and energy density from their inherent characteristics. MATLAB/ Simulink® based test bench is created by using different DC-DC converters for all energy storage devices and an inverter is modeled to supply the time varying load. The results provided by the EMS are highly satisfactory that proves its adaptability.

Keywords**—**Energy Management System (EMS) Fuel Cell, Ultracapacitor, Battery, Hybrid Energy Storage.

I. Introduction

WITH the growing concerns of the power requirements, the energy storage devices are finding their significant role in power systems. These devices have the capacity to store and deliver the energy as and when required. The Fuel Cell, Supercapacitor, and battery are some of the energy storage devices having different characteristics. These devices if managed by a well-designed energy management system can perform at their best to give the valid solution. The coordination of these devices as the hybrid energy storage can result in the best storage medium combining the unique characteristics of all of them. The primary role of an energy management in fuel cell based hybrid energy storage system is to decrease the consumption of the hydrogen and at the same time improving the dynamic behavior. The fuel the cell efficiency is directly related to the power load; that degrades at low power or very high transient power. Because of internal dynamics, the fuel cell transient response is somewhat sluggish [1]-[3]. In automotive and household application the load profile change in a wide range. Therefore, in most cases only fuel cell based systems may not work as an affirmative power source or an energy storage gadget. The ultracapacitor and battery combined with the fuel cell can resolve the above-listed problems. The ultracapacitors will work during high power density requirements, and the batteries can work for very low power requirements as well as during the regular power requirements. In this research work a Proton Exchange Membrane Fuel Cell (PEMFC) is combined with the ultracapacitor and the battery.

PEMFCs are specially developed for stationary and portable fuel cell applications. They work on the same principle of PEM electrolysis. Fig. 1 presents the basic working principle of the PEMFC. PEMFCs are made from Membrane Electrode Assemblies (MEA) that comprises electrodes, catalyst, gas diffusion layers, and electrolyte. The PEMFC converts the chemical energy released when the electrochemical reaction of oxygen and hydrogen to electrical energy. A current of hydrogen is transferred to the anode side of the membrane electrode assembly (MEA) [4], [5]. It is catalytically split into two parts viz. Electrons and Protons at the anode side. This Hydrogen Oxidation Reaction (HOR) is given by;

$$\text{At anode;} \quad H_2 \rightarrow 2H^+ + 2e^- \tag{1}$$

$$\text{At cathode;} \quad \tfrac{1}{2} O_2 + 2H^+ + 2e^- \rightarrow H_2O \tag{2}$$

$$\text{Overall;} \quad H_2 + \tfrac{1}{2} O_2 \rightarrow H_2O \tag{3}$$

The PEMFC operates at efficiency in the range of 40 - 60%. The ohmic, activation and mass transportation losses are the main culprits for a reduction in the efficiency.

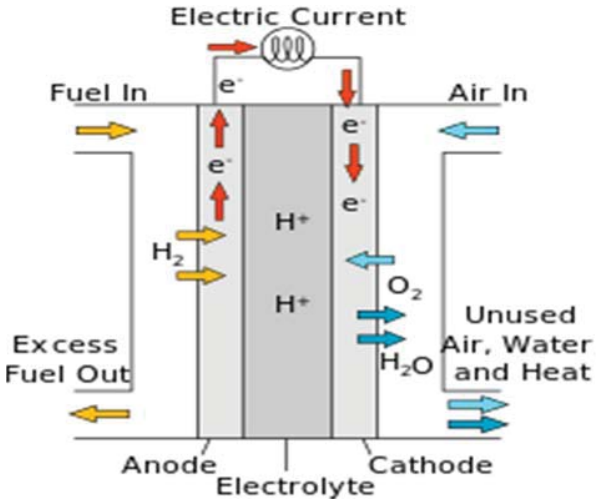

Fig. 1 Working of a fuel cell

Vinod Tejwani is Ph.D. Scholar at Gujarat Technological University (GTU), Ahmedabad Gujarat, India (e-mail: vstkeya@yahoo.com).

Dr. Bhavik Suthar is Associate Professor and Head of Electrical Engineering, L.D. College of Engineering, Ahmedabad, Gujarat, India.

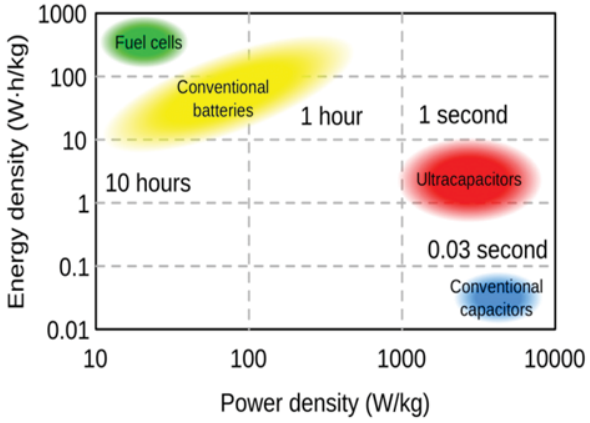

Fig. 2 Comparison of Energy Storage Technologies

The supercapacitors (SCs) are quickly emerging as future energy storage devices for the pulsed loads and hybrid electric vehicles. Their applications are ranging from small aircraft to trams and hybrid buses. The attractive feature of the supercapacitor (popularly known as the Ultracapacitor or UC) is its extremely high power density. Supercapacitor stores the energy electrostatically on the surface of the material that does not include chemical reactions [6]-[8]. These capacitors can be charged and discharged very quickly in comparison to the batteries or fuel cells. Table I presents the comparison of these three energy storage devices. Table I indicates that the supercapacitor has highest power density as well as highest recycle life in comparison to other two devices. Fig. 2 shows Ragone chart for a pictorial comparison of these energy storage devices. The fundamental deficiency of the supercapacitor is its lower energy density that indicates the smaller energy storage per gram of the material used. Batteries have better energy density. The fuel cell, the Supercapacitor, and the battery may be connected in parallel, to get the advantages of all storage technologies. This combination will be able to work with fast changing as well as steady load conditions. It can also work satisfactorily under peak or pulsed load situations. The controlling of the parallel combination has several issues related to it, and they are discussed in the subsequent section [9]-[15].

II. Hybridization of Three Energy Storage Elements

As discussed earlier, the hybridization will result in better system performance, but the essential concerns related to the hybridization are to be addressed at first.

Voltage Control at the DC Bus

For any hybrid energy storage, the voltage control at the DC bus is always a critical issue. If the voltage at the DC bus is not controlled accurately, it may result in the circulating currents and consequently, the heating of the energy stockpiling devices. Furthermore, the improper voltage at the DC bus may also affect the performance of the load. To controlled voltage at the DC bus, the proposed system is equipped with buck and boost converters at the appropriate places to be discussed the forthcoming section [16].

Battery and Supercapacitor SOC

The Depth of Discharge (DOD) or State of Charge (SOC) is an important indication of the health of the energy storage device, especially, the battery. If the battery SOC, goes below certain limit may result in shortening its life or the performance. The test bench created in the simulations have predefined limit of 50% for the battery SOC. The supercapacitors are not considerably affected by SOC, and its limit is kept to 25% for controlling the voltage level at the DC bus [17].

Higher Discharge Current for the Battery or Fuel Cell

The greater discharge current for the battery or the fuel cell can shorten the life of these devices. Studies at the V.V.P. Engineering College, Rajkot, Gujarat, India shows that discharging the battery of 5 Ah capacity at 2.5 A discharging current can make the battery inoperative. As the Fuel Cell has the lowest power density amongst these three energy storage devices, because of the inherent dynamics of it, asking for the higher discharging current than the specified, may result in the adverse effect on its life.

Battery Model

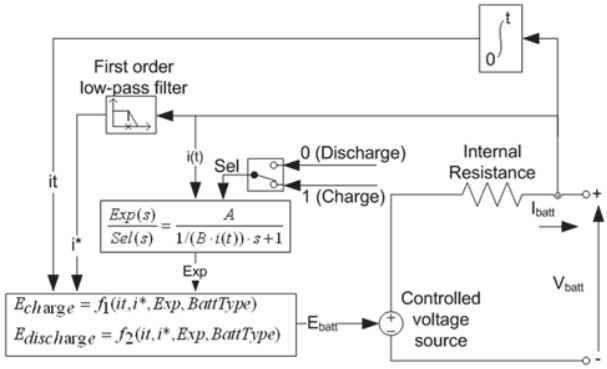

Fig. 3 Battery Model in Simulink

The battery model in the Simulink is presented in Fig. 3. For the Lithium –ion battery, the model equations are written as;

$$f_1(it, i^*, i) = E_0 - \frac{KQi*}{Q-it} - \frac{KQit}{Q-it} + A\cdot\exp(-B\cdot i_t) \quad (4)$$

$$f_2(it, i^*, i) = E_0 - \frac{KQi*}{it+0.1Q} - \frac{KQit}{Q-it} + A\cdot\exp(-B\cdot i_t) \quad (5)$$

where, E_0 = Constant voltage (V), K = Polarization constant (Ah^{-1}) or Polarization resistance (Ohms), Q = Maximum battery capacity (Ah), Sel(s) = Represents the battery mode, Sel(s) = 0 during battery discharge, Sel(s) = 1 during battery charging, i = Battery current (A), A = Exponential voltage (V), it = Extracted capacity (Ah), E_{Batt} = Nonlinear voltage (V), i* = Low frequency current dynamics (A), B = Exponential capacity $(Ah)^{-1}$, Exp(s) = Exponential zone dynamics (V).

Equation (1) is written for the discharge model and (2) for charge pattern of the battery. This model is a much know, developed by the MATLAB/Simulink® documentation center.

The model parameters used for various simulations are presented in Table I.

TABLE I
BATTERY MODEL PARAMETERS

Parameter	Value
Rated voltage	16 V
Rated Capacitance	291 F
Internal resistance	0.021 Ohm
Surge Voltage	17 V
Leakage current	5.2 mA
Operating temperature	25 Deg. celsius

TABLE II
SUPERCAPACITOR MODEL PARAMETERS

Parameter	Value
Rated voltage	48 V
Rated Capacity	40 Ah
Fully charged voltage	55.87 V
Initial SOC	65 %
Nominal discharge current	17. 4 A
Internal resistance	12 mΩ

Following assumptions are made for the Simulink battery model.

(a) During the charge and discharge cycles for the battery, its internal resistance remains constant.
(b) The capacity of the battery doesn't change with the magnitude of the current, as Peukert effect is not considered.
(c) The memory effect of the battery is not accounted for.
(d) Temperature variations are not given any attention, i.e. the considered model is temperature independent.

Taking these assumptions into account, the State of Charge (SOC) for the battery model is computed using the equation;

$$\text{SOC} = 100\left(1 - \frac{1}{Q}\int_0^t i(t)dt\right) \tag{6}$$

Supercapacitor Model

The supercapacitor (SC) model considered in test bench simulations is the most popular SC model given by Stern-Tafel. The model equations are given by;

$$\text{V}=\frac{NNsQX2}{NNpN\text{^}2\varepsilon\varepsilon 0A}+\frac{NNs2RT}{F}\alpha\cdot r\cdot\sinh\left(\frac{Q}{NpN^{2A}\sqrt{8RT\varepsilon\varepsilon 0c}}\right) \tag{7}$$

$$-i_c(t) = Ai_0 \exp\left(\frac{\alpha F\left(\frac{V}{Ns}-\frac{Vmax}{Ns}\Delta V\right)}{RT}\right) \tag{8}$$

where, x2 = Helmholtz layer length (m), α = Charge transfer coefficient, Tafel equation (0<alpha<1), NA= Avogadro constant, Q = Electric charge (C), R= Ideal gas constant , Np = Number of parallel supercapacitors, Ns = Number of series supercapacitors, A= Interfacial area between electrodes and electrolyte (m^2), C = Molar concentration (mol m^{-3}) equal to c = $0.86/(8NAr^3)$, ΔV = Over potential,i = Current density (Am^{-2}), if = Leakage current (A), k =Stefan-Boltzmann constant, N = Number of layers of electrodes, r = Molecular radius equal x2, i0 = Exchange current density, i0 = if/A (Am^{-2}), ε = Permittivity of material, F = Faraday constant, ε0 = Permittivity of free space

The parameters of the supercapacitor considered for various tests are presented in Table II.

Few assumptions are made while considering the supercapacitor model.

(a) The capacitance and the internal resistance of the supercapacitor remain constant during the charge and discharge cycles.
(b) The model considered for tests is temperature independent.
(c) Cell balancing is not implemented
(d) The current passing through the Sc is continuous.
(e) The charge redistribution remains same irrespective of the voltage or current magnitude.

Taking these assumptions into account, the State of Charge (SOC) for the supercapacitor is calculated by (9).

$$\text{SOC} = \frac{\text{Qinit}-\int_0^t \text{i}(\tau)\,\text{d}\tau}{\text{QT}} \times 100 \tag{9}$$

Fuel Cell Model

The fuel cell model taken into consideration for the test bench is presented in Fig. 4. For this model, the equations are written as;

$$E_{oc} = K_c\, E_n \tag{10}$$

$$\text{i}_0 = \frac{\text{zFk (PH2+Po2)}}{\text{Rh}} \text{e}^{\frac{-\Delta G}{RT}} \tag{11}$$

$$\text{A} = \frac{RT}{z\alpha F} \tag{12}$$

where, R = 8.3145 J/(mol K), z = Number of moving electrons, PH2 = Partial pressure of hydrogen inside the stack (atm), k = Boltzmann's constant = 1.38 × 10–23 J/K, h = Planck's constant = 6.626 × 10–34 J s, ΔG = Size of the activation barrier which depends on the type of electrode and catalyst used, F = 96485 A s/mol, T = Temperature of operation (K), En = Nernst voltage, which is the thermodynamics voltage of Kc = Voltage constant at nominal condition of operation, α = Charge transfer coefficient, which depends on the type of electrodes and catalysts used, PO2 = Partial pressure of oxygen inside the stack (atm).

The conversion rates of hydrogen utilization (UfH2) and oxygen (UfO2) are determined as;

$$\text{U}_{\text{fH2}} = \frac{(\text{n\^r})\text{H2}}{(n^{in})O2} = \frac{60000\,RTNifc}{zFPfuelVipmX\%} \tag{13}$$

$$\text{U}_{\text{fo2}} = \frac{(\text{n\^r})\text{o2}}{(n^{in})O2} = \frac{60000\,RTNifc}{zFPfairVipm(air)\,y\%} \tag{14}$$

where, Pfuel = Absolute supply pressure of fuel (atm), Pair = Absolute supply pressure of air (atm), Vlpm(fuel) = Fuel flow rate (l/min), Vlpm(air) = Air flow rate (l/min), x = Percentage of hydrogen in the fuel (%), y = Percentage of oxygen in the oxidant (%), N = Number of cells.

The various parameters for the fuel cell are presented in Table III. Fig. 5 shows the fuel cell (FC) dynamics based on the above equations.

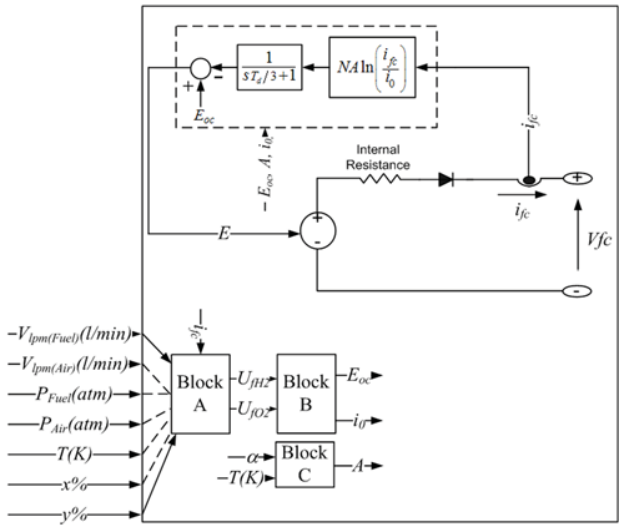

Fig. 4 Fuel cell model

TABLE III
FUEL CELL PARAMETERS

Parameter	Value
Voltage at 0 A	52.5 V
Nominal operating current (Inom)	250 A
Nominal operating voltage	41.15 V
Maximum operating current	320 A
Minimum operating voltage	39.2 V
Nominal stack efficiency	50 %
Nominal air flow rate	732 lpm
Operating temp	45 Deg. Celsius
Nominal supply pressure of fuel	1.16 bar
Maximum stack power	12.5 kW
Exchange coefficient (alpha)	0.9455
Internal resistance	0.02455 ohm
Fuel cell response time	1 Second

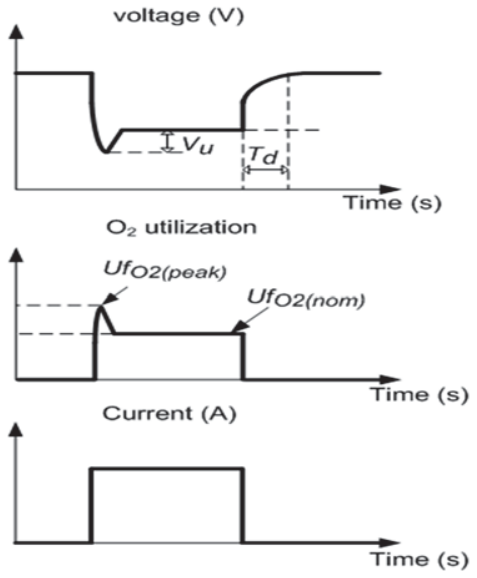

Fig. 5 FC Dynamics

Considering the battery, supercapacitor, and fuel cell model the control strategy was formulated for the hybrid source containing all three sources.

III. Control Strategy for the Hybrid Energy Storage

The control strategy for the hybrid energy storage is aimed to manage the energy consumption of the hydrogen fuel and at the same time, the pulsed or transient power required by the load should be supplied. A Fuel cell is controlled by boost converter, battery, and supercapacitor by buck-boost DC-DC converters.

Boost Converter for the Fuel Cell

The DC-DC boost converter controls the fuel cell. Fig. 6 presents the converter topology.

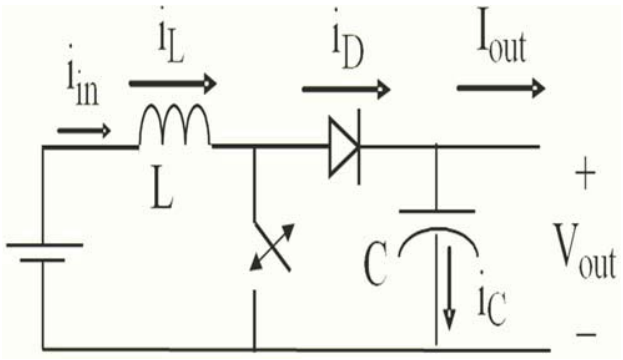

Fig. 6 Boost converter for the battery

For Fig. 6, peak inductor current = i_{pk}, Minimum inductor current = i_o, ripple current = $\Delta i = i_{pk} - i_o$, off duty cycle = 1-D = T_{off}/T, switching off time = T_{off} = (1-D)/f, ripple current to average current = $\Delta i/i_{av}$, RMS current for a triangular wave = $\sqrt{io^2 + (\Delta i)^2/12}$

The relationship between the current and the voltage can be written as;

$$V = L\frac{di}{dt} \tag{15}$$

$$i = \frac{1}{L}\int_0^t V dt + i_o \tag{16}$$

When the switch is on;

$$i_{pk} = \frac{(Vout - Vin)Ton}{L} \tag{17}$$

$$\Delta i = \frac{(Vin - VTmos)Ton}{L} \tag{18}$$

When the switch is off;

$$i_o = i_{pk} = \frac{(Vout - Vin + VD)Toff}{L} \tag{19}$$

or

$$\Delta i = \frac{(Vout - Vin + VD)Toff}{L} \tag{20}$$

where, V_D represents the voltage drop across the diode, Vmos is the voltage drop across the MOSFET (Switch) and at current i_o is zero, the continuous/discontinuous mode boundary will occur.

Equating for Δi, we can find out the solution for V_{out} as,

$$V_{out} = \frac{Vin - Vmos*D}{(1-D)} - V_D \quad (21)$$

If the voltage drops across the diode and MOSFET is neglected, the above equations are written as;

$$V_{out} = \frac{Vin}{(1-D)} \quad (22)$$

These equations imply that if the duty cycle D is chosen suitably, then boost function of the converter will give the accurate results.

Inductor Design for the Boost Converter

In the equations derived above, it is seen that the inductance is inversely proportional to the magnitude of ripple current. The inductor design thus becomes an important parameter to reduce the ripple currents. The test bench used for the simulations has inductance 1 mH that assures the continuous flow of the current.

Buck-Boost Converter for the Battery and Supercapacitor

Bi-directional DC-DC buck-boost converter controls the battery and supercapacitor. Charging and discharging of both the gadgets is possible with this configuration. This action of charging or discharging is conducted at the required voltage by fitly controlling the duty cycle D.

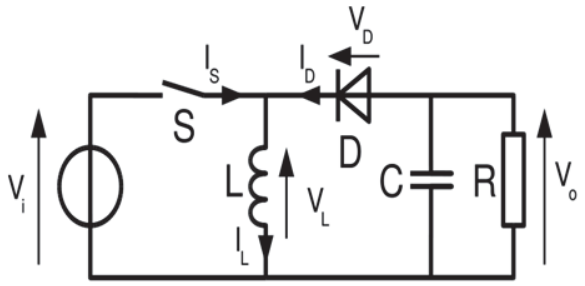

Fig. 7 Buck -Boost converter for the battery & supercapacitor

For buck boost converter of the Fig. 7,

I_L = Load current, On = On-time, D = Duty cycle, V_i = input voltage, V_o = output voltage

When the switch S is in on-state, the inductor current will change and its rate of change is indicated as,

$$\frac{dIL}{dt} = \frac{Vi}{L} \quad (23)$$

At the end of the On-state, the change in inductor current is written as,

$$\Delta I_{Lon} = \int_0^{DT} dIL = \int_0^{DT} \frac{Vi}{L} dt = \frac{ViDT}{L} \quad (24)$$

During the off state of the switch S, the inductor current will flow through the load. Assuming zero voltage drop in the diode and large capacitor enough to make voltage constant, the equation for the I_L is written as,

$$\frac{dIL}{dt} = \frac{Vo}{L} \quad (25)$$

Therefore, the variation of I_L in the off-period is,

$$\Delta I_{Loff} = \int_0^{(1-D)T} dIL = \int_0^{(1-D)T} \frac{Vo}{L} dt = \frac{Vo(1-D)T}{L} \quad (26)$$

In the steady state action of the converter, the quantity of energy in the converter elements will be identical at the commencement and end of the commutation cycle. Therefore,

$$E = \frac{1}{2} LI_L^2 \quad (27)$$

It is evident that the sum of changes in I_L for on-state and off-state should be zero. Hence,

$$\Delta I_{Lon} + \Delta I_{Loff} = 0 \quad (28)$$

Substituting the equations of ΔI_{Lon} and ΔI_{Loff},

$$\Delta I_{Lon} + \Delta I_{Loff} = \frac{ViDT}{L} + \frac{Vo(1-D)T}{L} = 0 \quad (29)$$

That can be presented as,

$$\frac{Vo}{Vi} = \frac{D}{D-1} \quad (30)$$

$$D = \frac{Vo}{Vo-Vi} \quad (31)$$

The relationship between Vo and Vi shows that by managing the duty cycle, one can buck or boost the input voltage in the output. The inductor is designed in a similar way to the boost converter of the fuel cell, and again it is considered as 1 mH.

The complete energy management system for the Fuel Cell Hybrid Power Generation (FCHPG) is presented in Fig. 8. The inverter, supplying the load is rated at 270 V DC in, 200V AC out, 400 Hz, 15 kVA. A 3 phase load profile is emulated to consider variations in power at the different timings and simulations are worked upon to see the behavior of the hybrid energy storage system as a whole and the response of each storage device.

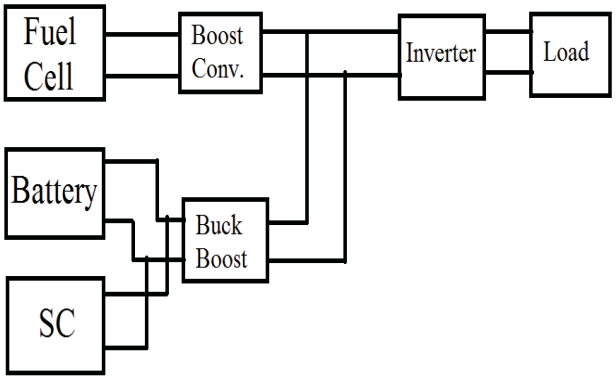

Fig. 8 Energy management system for FCHPG

IV. Results and Discussion

As discussed earlier, a test bench comprising of the load profile and the energy storage devices with the appropriate converters to manage the energy flow was created in MATLAB/ Simulink® environment to evaluate the performance of the hybrid energy storage system. The set of curves are presented in Figs. 9 (a) to 9 (a6), 9 (b1) to 9 (b5) and 9 (c1) to 9 (c2). These set of curves prove the adaptability of the presented hybrid energy control system. Fig. 9 (a) indicates the load power variations (required power) that change quite frequently. With these changes, the fuel cell action is presented from Figs. 9 (a1)-(a6). As the fuel cell is supplying the load, its voltage decreases to 51.2 Volts, and it remains constant for the whole simulation time of 350 seconds. Figs. 9 (a2), (a3) and (a4) show that the fuel cell current, power and fuel consumption (lpm) nearly remains constant with the highly changing load power requirements. The transient power is mostly supplied by the Supercapacitor, and a part of power is furnished by the battery also. Figures also conclude that the battery power, battery voltage and current are almost steady, and the energy management system works nicely. Without the energy management if the fuel cell is implemented, either it will not be able to supply the transient load due to the higher requirement of the power density or the battery would get the deep discharge. Here is the exact role of the energy management system to prevent the fuel consumption of fuel cell to optimum, and at the same time, battery life is preserved.

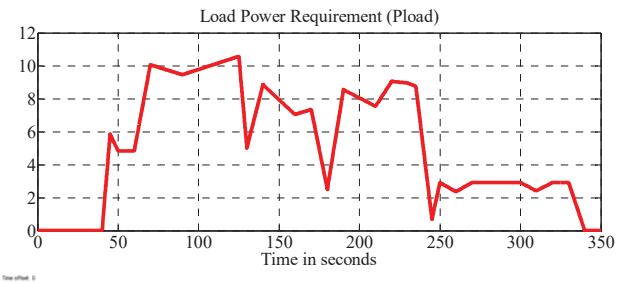

Fig. 9 (a) Load power required

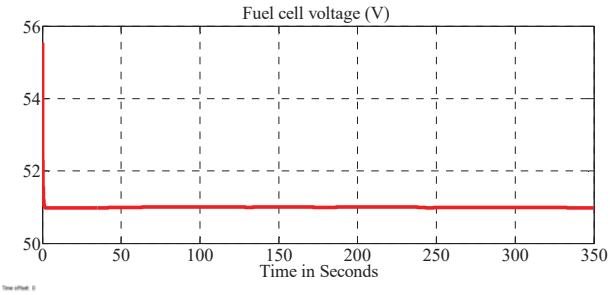

Fig. 9 (a1) Fuel cell voltage variation

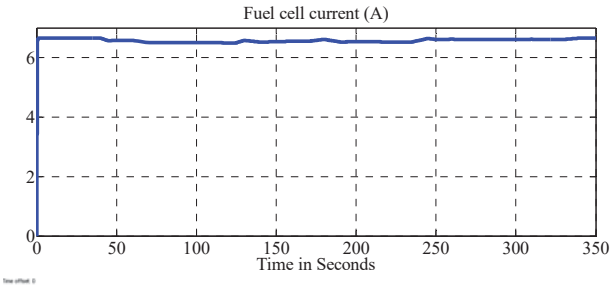

Fig. 9 (a2) Fuel cell current variation

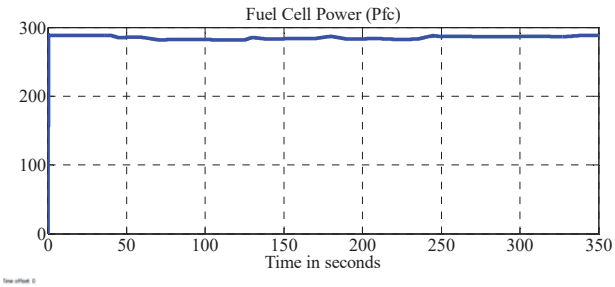

Fig. 9 (a3) Fuel cell power variation

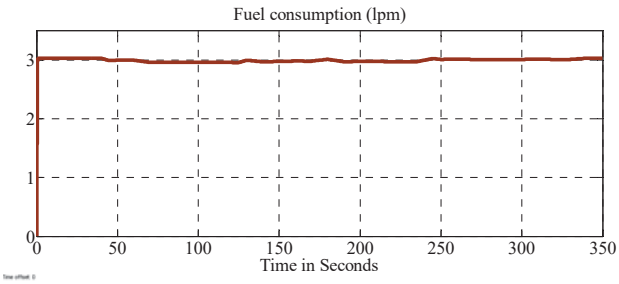

Fig. 9 (a4) Fuel consumption (lpm)

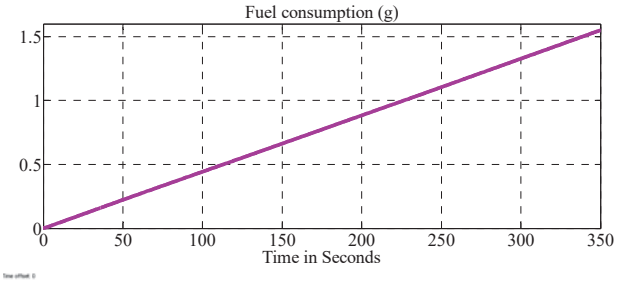

Fig. 9 (a5) Fuel consumption (g)

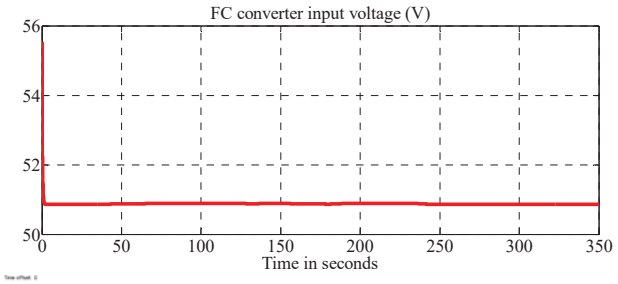

Fig. 9 (a6) Fuel cell converter input voltage variation

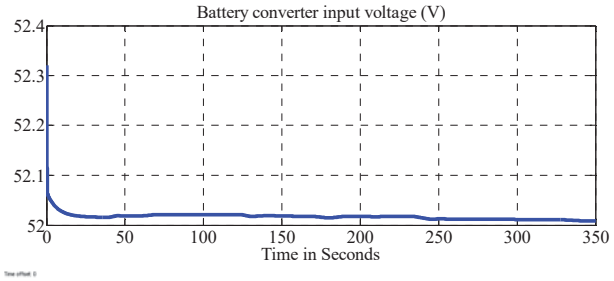

Fig. 9 (b1) Battery converter input voltage variation

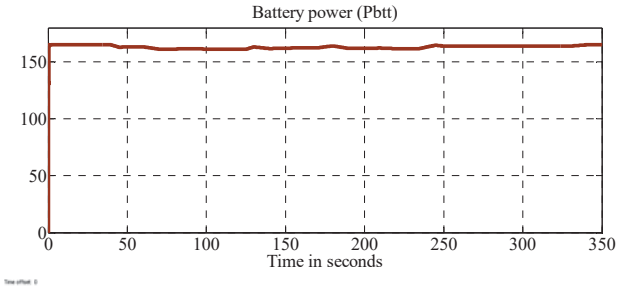

Fig. 9 (b2) Battery power variation

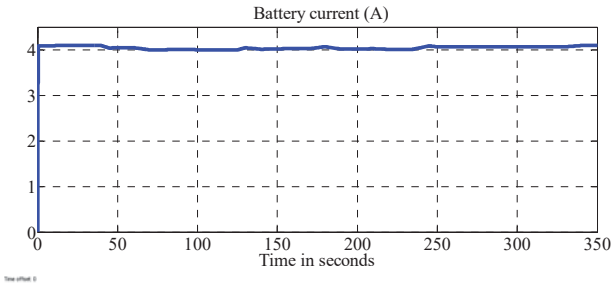

Fig. 9 (b3) Battery current variation

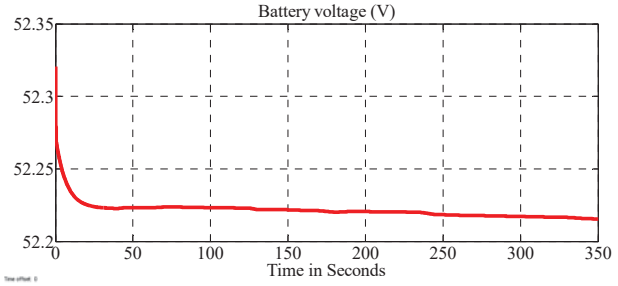

Fig. 9 (b4) Battery voltage variation

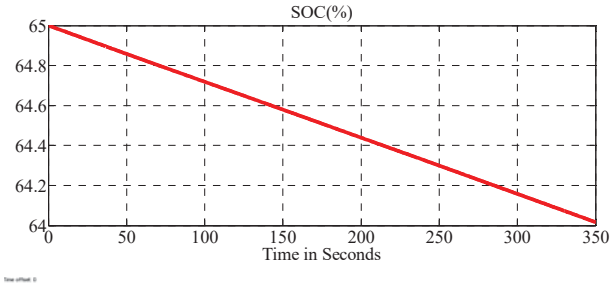

Fig. 9 (b5) Battery SOC variation

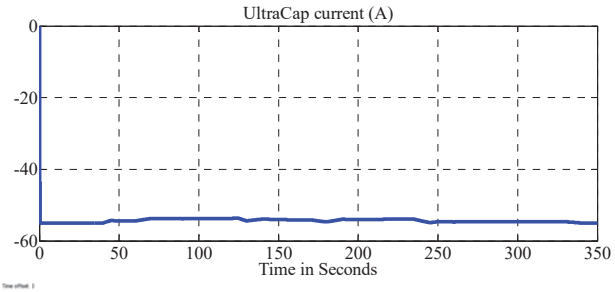

Fig. 9 (c1) Supercapacitor current variation

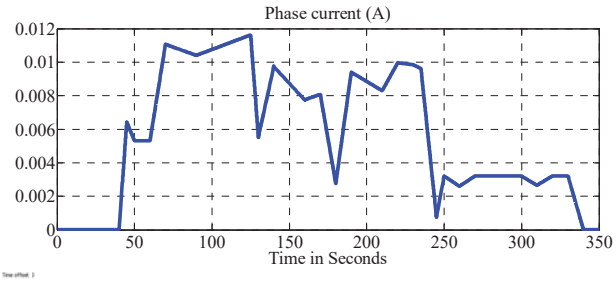

Fig. 9 (c2) Load phase current variation

Case 2

A similar case as discussed for the set of figures (Figs. 9 (a)-(c2)) is simulated for the different load power requirements and the results are presented in a set of figures (Figs. 10 (a)-(c2)). These figures also prove the same fact that the fuel consumption in the fuel cell is largely steady and optimum, the battery is working in the safe zone the most of the transient power is supplied by the supercapacitor. This again shows that the whole energy management system works fine.

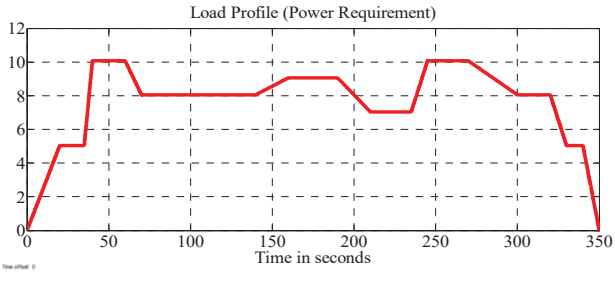

Fig. 10 (a) Load power required

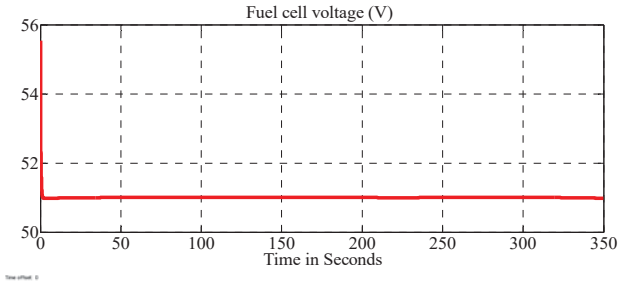

Fig. 10 (a1) Fuel cell voltage variation

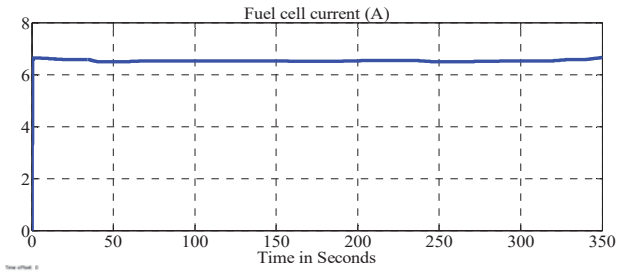

Fig. 10 (a2) Fuel cell current variation

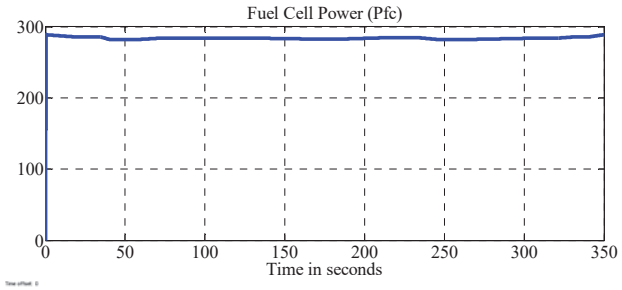

Fig. 10 (a3) Fuel cell power variation

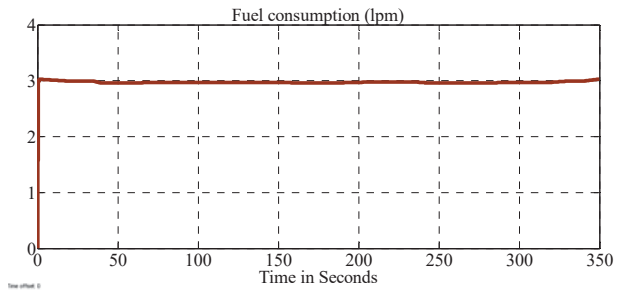

Fig. 10 (a4) Fuel consumption (lpm)

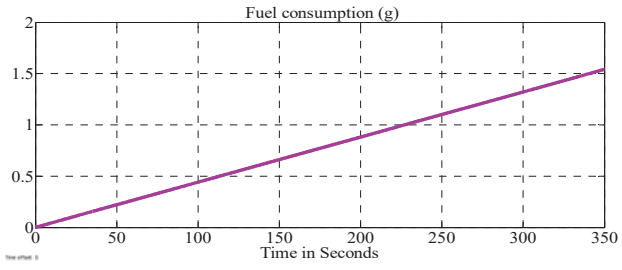

Fig. 10 (a5) Fuel consumption (g)

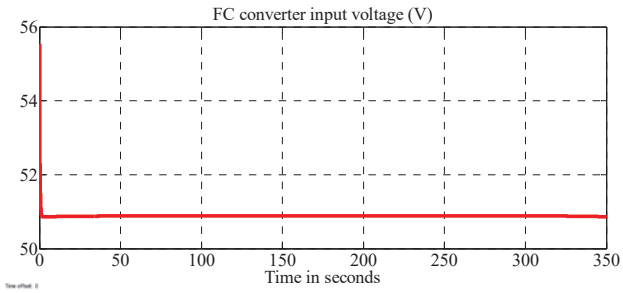

Fig. 10 (a6) Fuel cell converter input voltage variation

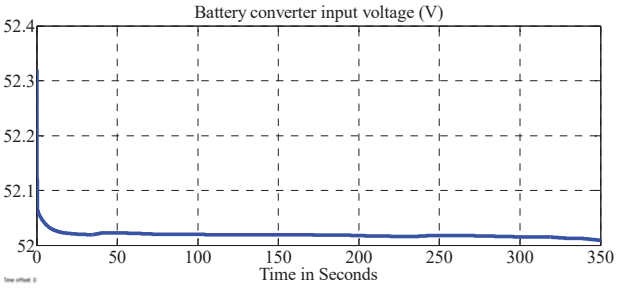

Fig. 10 (b1) Battery converter input voltage variation

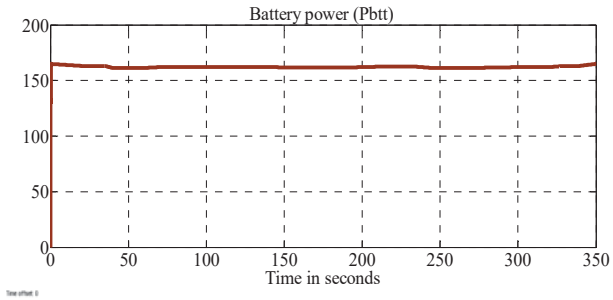

Fig. 10 (b2) Battery power variation

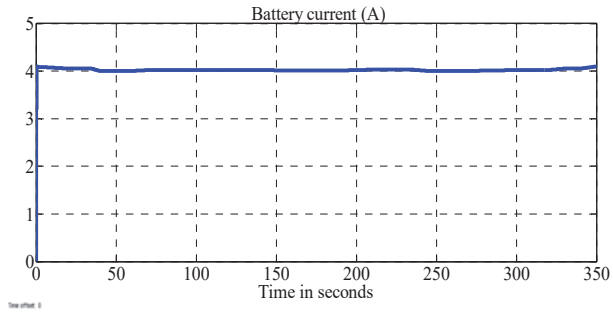

Fig. 10 (b3) Battery current variation

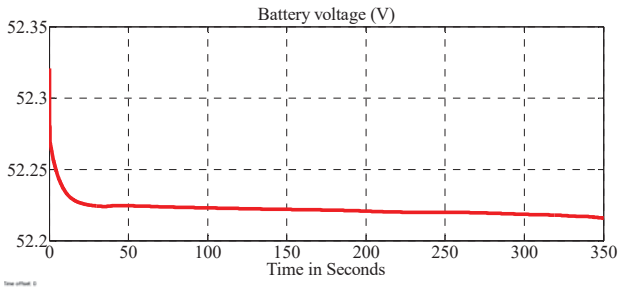

Fig. 10 (b4) Battery voltage variation

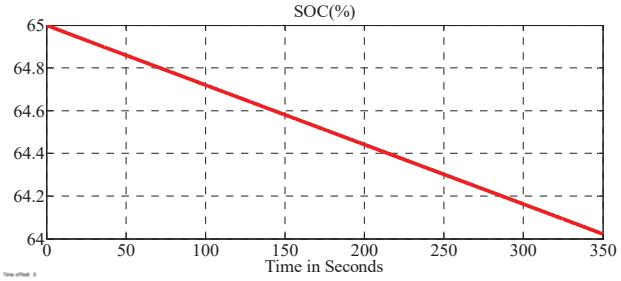

Fig. 10 (b5) Battery SOC variation

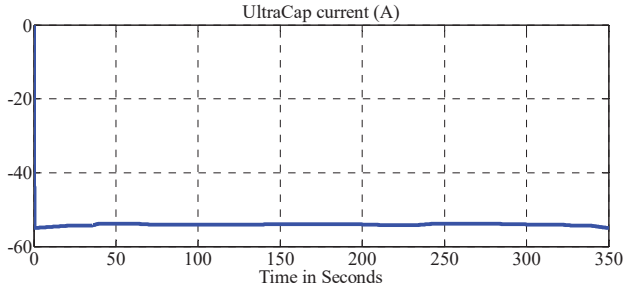

Fig. 10 (c1) Supercapacitor current variation

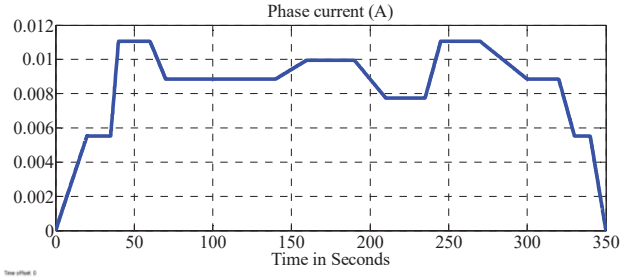

Fig. 10 (c2) Load phase current variation

V. Conclusion

The paper demonstrates energy management system for the fuel cell hybrid power generation (FCHPG). The energy management system is implemented in MATLAB/Simulink test bench. The different load profiles were created to study the response of three different energy storage devices. The energy management system proposed works well and it can be used for the applications with the pulsed loads and high transient power requirements. The control strategy determined by various DC-DC converters ensured that the Supercapacitor chiefly supplied the temporal power and the steady power is furnished by the fuel cell and the battery. Thus, the fuel cell fuel consumption is made optimum and the battery life is prolonged.

References

[1] Suhadiyana Hanapi, Alhassan Salami Tijani, W. A. N Wan Mohamed, "Influence on Driving Strategy on Power and Fuel Consumption of Lightweight PEM Fuel Cell Vehicle Powertrain" *World Academy of Science, Engineering and Technology, International Journal of Electrical, Computer, Energetic, Electronic and Communication Engineering* Vol:10, No:1, pp. 12-18, 2016.

[2] Abdar Ali, Rizwan Ullah, Zahid Ullah, "DC-to-DC Converters for Low-Voltage High-Power Renewable Energy Systems" *World Academy of Science, Engineering and Technology, International Journal of Electrical, Computer, Energetic, Electronic and Communication Engineering* Vol:9, No:12, pp.1299-1304, 2015.

[3] Kevser Dincer, Basma Waisi, M. Ozan Ozdemir, Ugur Pasaogullari, Jeffrey McCutcheon, "Experimental Investigation of Proton Exchange Membrane Fuel Cells Operated with Nanofiber and Nanofiber/ Nanoparticle" *World Academy of Science, Engineering and Technology, International Journal of Electrical, Computer, Energetic, Electronic and Communication Engineering* Vol:9, No:12, pp.1367-1371, 2015.

[4] Fatma Keskin Arabul, Ibrahim Senol, Ahmet Yigit Arabul, Ali Rifat Boynuegri, "Providing Energy Management of a Fuel Cell-Battery Hybrid Electric Vehicle" *World Academy of Science, Engineering and Technology, International Journal of Electrical, Computer, Energetic, Electronic and Communication Engineering* Vol:9, No:8, pp.920-924, 2015.

[5] Abdolreza Roozbeh, Reza Sedaghati, Ali Asghar Baziar, Mohammad Reza Tabatabaei, "Dynamic Performance Evaluation of Distributed Generation Units in the Micro Grid" *World Academy of Science, Engineering and Technology, International Journal of Electrical, Computer, Energetic, Electronic and Communication Engineering* Vol:9, No:2, pp.550-554, 2015.

[6] Oldham, K. B. "A Gouy-Chapman-Stern model of the double layer at a (metal)/(ionic liquid) interface." *J. Electroanalytical Chem.* Vol. 613, No. 2, pp. 131–38, 2008.

[7] Xu, N., and J. Riley. "Nonlinear analysis of a classical system: The double-layer capacitor." *Electrochemistry Communications*. Vol. 13, No. 10, pp. 1077–1081, 2011.

[8] Phatiphat Thounthong, Stephane Raël, Bernard Davat, "Energymanagementoffuelcell/battery/supercapacitorhybridpowersource for vehicle applications", *Journal of Power Sources* Vol.193, pp.376–385, 2009.

[9] Tremblay, O., Dessaint, L.-A. "Experimental Validation of a Battery Dynamic Model for EV Applications." *World Electric Vehicle Journal*, Vol.3, 2009.

[10] K. Yoshimoto, T. Nanahara, G. Koshimizu, "New Control Method for Regulating State-of- Charge of a Battery in Hybrid Wind Power/Battery Energy Storage System," *IEEE PES Power Systems Conference and Exposition, PSCE '06*, Oct. 2006, pp. 1244 – 1251.

[11] P.F. Ribeiro, B.K. Johnson, M.L. Crow, A. Arsoy, Y. Liu, "Energy storage systems for advanced power applications," *Proceedings of the IEEE*, Vol. 89, Issue 12, pp. 1744 – 1756, 2001.

[12] S.A. Lone, and M.-u-D. Mufti, "Integrating a Redox Flow Battery System with a Wind-Diesel Power System," *International Conference on Power Electronics, Drives and Energy Systems, PEDES '06*, pp.1–6, 2006.

[13] J. Chahwan, C. Abbey, M. Chamberland, G. Joos, "Battery Storage System Modelling, Design and Operation for Wind Energy Integration in Power Systems," *CIGRE Canada Conference on Power Systems*, 2007.

[14] A. Arulampalam, M. Barnes, N. Jenkins, J.B. Ekanayake, "Power quality and stability improvement of a wind farm using STATCOM supported with hybrid battery energy storage," *IEE Proceedings of Generation, Transmission and Distribution*, Vol. 153, No. 6, pp.701–710, 2006.

[15] M. -H. Li, T. Funaki and T. Hikihara, "A Study of Output Terminal Voltage Modeling for Redox Flow Battery Based on Charge and Discharge Experiments", *Fourth Power Conversion Conference*, pp.221-225, 2007.

[16] Vinod S. Tejwani, Bhavik N Suthar "Novel Control Strategy for Grid-connected PVES for Smart Distribution System" *Fifth International Conference on Power and Energy Systems*, Kathmandu, Nepal, 2013.

[17] Vinod S. Tejwani, Bhavik N Suthar and Denish A. Prajapati, "Integration of Microgrid with Utilitygrid for sharing Real and Reactive Power" *IEEE International Conference on Computer, Communication and Control (IC4-2015)*, Indore, M.P, INDIA,2015.